Metal-organic frameworks with high capacity and selectivity for harmful gases

David Britt, David Tranchemontagne, and Omar M. Yaghi*

Department of Chemistry and Biochemistry, Center for Reticular Materials Research at California NanoSystems Institute, University of California, Los Angeles, CA 90095

Edited by Jack Halpern, University of Chicago, Chicago, IL, and approved June 16, 2008 (received for review May 20, 2008)

Benchmarks have been established for the performance of six metal-organic frameworks (MOFs) and isoreticular MOFs (IRMOFs, which have the same underlying topology as MOF-5), MOF-5, IRMOF-3, MOF-74, MOF-177, MOF-199, and IRMOF-62, as selective adsorbents for eight harmful gases: sulfur dioxide, ammonia, chlorine, tetrahydrothiophene, benzene, dichloromethane, ethylene oxide, and carbon monoxide. Kinetic breakthrough measurements are used to determine the calculated dynamic adsorption capacity of each ''benchmark'' MOF for each gas. The capacity of each MOF is compared to that of a sample of Calgon BPL activated carbon. We find that pore functionality plays a dominant role in determining the dynamic adsorption performance of MOFs. MOFs featuring reactive functionality outperform BPL carbon in all but one case and exhibit high dynamic adsorption capacities up to 35% by weight.

air purification | dynamic adsorption | reticular chemistry

Release of harmful chemicals into our environment is a growing national security concern. A number of industrial chemicals produced in excess of 1 million tons/year worldwide are also highly toxic and can be obtained with relative ease. Effective capture of these chemicals is of great importance both to the protection of the environment and to those who are at risk for being exposed to such materials (1). General-purpose filters are often composed of activated carbon impregnated with copper, silver, zinc, and molybdenum salts (2). Although such filters have proven to be effective in containing a range of toxic gases, they are not adequately effective against all potential threats (3, 4). The current applications of activated carbons and any needed improvements on its current performance are largely limited by lack of control over the metrics and functionality of the pores because of the highly amorphous nature of its carbon network. Such obstacles must be overcome if materials are to be developed to address any conceivable harmful chemical.

Metal-organic frameworks (MOFs) are a new class of crystalline porous materials, the structure of which is composed of metal-oxide units joined by organic linkers through strong covalent bonds (5, 6). The flexibility with which these components can be varied has led to an extensive class of MOF structures with ultrahigh surface areas, far exceeding those achieved for porous carbons (5, 7–9). They exhibit high thermal stability, with decomposition between 350°C and 400°C in the case of MOF-5 (10), ensuring their applicability across a wide temperature range. The unprecedented surface area and the control with which their pore metrics and functionality can be designed provide limitless potential for their structure to be tailored to carry out a specific application, thus suggesting the possibility of being superior to activated carbons in many applications.

Although application of MOFs to high-density gas storage has been well studied (11–19), virtually no work has been undertaken to measure their capacity for dynamic gas-adsorption properties. Equilibrium adsorption does not adequately predict selectivity, because dynamic capacity is influenced strongly by the kinetics of adsorption (4, 20). The kinetic properties of adsorption in MOFs have been largely unexamined. For these reasons it is necessary to calculate the dynamic adsorption capacity, which is defined as the quantity of a gas adsorbed by a material before the time at which the concentration of the gas in the effluent stream reaches an arbitrary ''breakthrough'' value, 5% of the feed concentration in this study. Here we report a series of dynamic adsorption experiments that establish benchmarks for adsorption capacity in MOFs across a range of contaminant gases and vapors. These benchmark adsorption values will serve to rate the potential of MOFs as a class of materials and as a comparison for future studies. Furthermore, they will provide insight into what properties of MOFs make them most suited as dynamic adsorption media.

The eight ''challenge'' gases were selected to include several for which activated carbons have poor uptake, such as ammonia and ethylene oxide, as well as several for which they have good uptake, such as chlorine and benzene. Also chosen were carbon monoxide, sulfur dioxide, dichloromethane, and tetrahydrothiophene. We sample a wide range of size, acidity, vapor pressure, and other variables to span the entire breadth of potential hazards. In a similar manner, six MOFs (Fig. 1) were chosen to explore a range of surface area, functionality, and pore dimensions, including MOFs with Brunauer, Emmett, and Teller (BET) surface areas ranging from $<$1,000 m^2/g to $>$4,000 m^2/g. We have also represented various functionalities, such as amines, aromatics, and alkynes, coordinatively unsaturated metal sites, and framework catenation, as outlined in Table 1. The dynamic adsorption capacities of the MOFs have been compared in each case to a sample of Calgon BPL carbon, a common undoped activated carbon that is used in various doped forms for many protective applications. An undoped carbon was chosen to establish a frame of reference for the MOFs, which are in themselves undoped. We find that for each gas there is a MOF with equal or greater, in some cases far greater, dynamic adsorption capacity. In particular, MOF-199 (HKUST-1) matches or outperforms BPL carbon in all but one case.

Results and Discussion

Capture of Gaseous Contaminants. Breakthrough curves for SO_2, NH_3, Cl_2, and CO adsorption in MOF-5, IRMOF-3, IRMOF-62, MOF-74, MOF-177, MOF-199 (the benchmark MOFs), and BPL carbon were recorded. Selected plots of breakthrough curves and estimated dynamic adsorption capacities for gaseous contaminants are presented in Fig. 2 and Table 2, respectively. No significant retention of carbon monoxide was observed for any of the materials. Carbon monoxide breakthrough curves do

Author contributions: D.B. and D.T. designed research; D.B. performed research; D.B. analyzed data; and D.B. and O.M.Y. wrote the paper.

The authors declare no conflict of interest.

This article is a PNAS Direct Submission.

*To whom correspondence should be addressed. E-mail: yaghi@chem.ucla.edu.

This article contains supporting information online at www.pnas.org/cgi/content/full/0804900105/DCSupplemental.

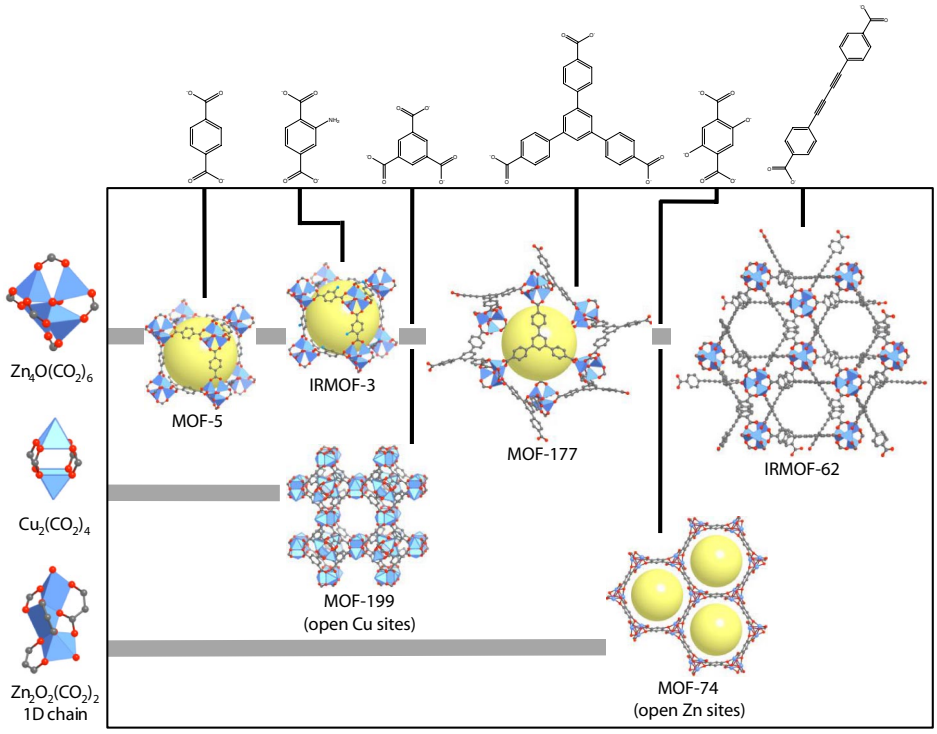

Fig. 1. The single-crystal x-ray structures of the benchmark MOFs: the $Zn_4O(CO_2)_6$ cluster linked by terephthalate (MOF-5), 2-aminoterephthalate (IRMOF-3), benzene-1,3,5-tris(4-benzoate) (MOF-177), and diacetylene-1,4-bis(4-benzoic acid) (IRMOF-62); the $Cu_2(CO_2)_4$ cluster linked by trimesate (MOF-199); and 1D $Zn_2O_2(CO_2)_2$ chains linked by 2,5-dihydroxyterephthalate (MOF-74). C atoms are represented in gray, O atoms are red, N atoms are teal, and metal ions are shown as blue polyhedra. H atoms were omitted for clarity. See Table 1 for additional structural information.

not differ from the curve measured for a blank sample cell and have been omitted for clarity.

We find retention of ammonia in all of the benchmark MOFs to be a vast improvement relative to BPL carbon, with three of the MOFs (IRMOF-3, MOF-74, and MOF-199) attaining at least 59-fold improvement in dynamic adsorption capacity. However, for all other gases, MOF-5 and MOF-177 exhibit markedly worse dynamic capacity than BPL carbon despite having higher surface area than all other materials tested. The lack of reactive functionality paired with the open, highly connected pore structure is, therefore, thought to make for an ineffective dynamic adsorption medium. Indeed, simply adding an amino functionality to the MOF-5 structure, which results in the IRMOF-3 structure, is sufficient to increase dynamic ammonia capacity more than 18-fold. Although IRMOF-62 has some kinetic adsorption capacity, it too lacks any reactive functionality and is surpassed by BPL carbon in almost all cases. All three of the aforementioned MOFs had little or no capacity for sulfur dioxide. The only MOF to have demonstrated considerable capacity for chlorine gas is IRMOF-62, which is likely the result of the highly reactive nature of the gas. Even in that case, BPL carbon is the more successful adsorbent. Despite their high capacities for thermodynamic gas adsorption, it is clear that MOFs lacking reactive adsorption sites are ineffective in kinetic gas adsorption.

Coordinatively unsaturated metal sites are known to be reactive as Lewis acids (21). They demonstrate efficacy as adsorption sites in testing of MOF-199 and MOF-74. MOF-199, which contains an open copper(II) site, outperforms BPL carbon by a factor of 59 in ammonia adsorption and performs equally well in adsorbing sulfur dioxide. MOF-74 is even more effective, adsorbing >62 times the amount of ammonia and nearly 6 times the

Table 1. Diverse characteristics of the benchmark MOFs

MOF	SBU* 0D	SBU* 1D	Open metal sites†	Functionalized pore‡	Catenated§	Ultrahigh surface area	Surface area, m^2/g¶	Pore volume, cm^3/g
MOF-5	■					■	2,205	1.22
IRMOF-3	■			■			1,568	1.07
MOF-74		■	■				632	0.39
MOF-177	■					■	3,875	1.59
MOF-199	■		■				1,264	0.75
IRMOF-62	■			■	■		1,814	0.99

*Secondary building units (SBUs) are either discreet inorganic clusters (0D) or linear chains (1D).
†MOF-74 contains pyramidal 5-coordinate zinc, and MOF-199 contains square 4-coordinate copper.
‡IRMOF-3 contains amino functionality, and IRMOF-62 contains alkyne functionality.
§IRMOF-62 is quadruply interpenetrated.
¶Surface areas calculated by the BET method for samples used in this study. These may differ from reported values as a result of variation in handling and activation procedures.

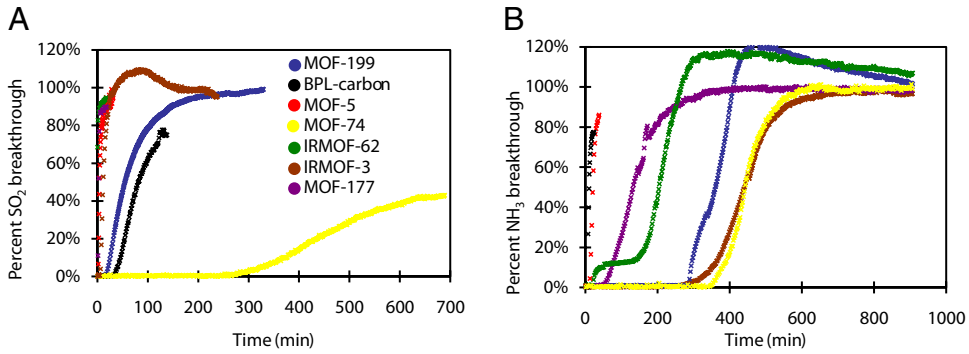

Fig. 2. Selected kinetic breakthrough curves of gaseous SO_2 (*A*) and NH_3 (*B*) contaminants in the benchmark MOFs. For breakthrough curves of other gases tested see supporting information (SI) Figs. S1 and S2.

amount of sulfur dioxide as the activated carbon sample. In both cases, the highly reactive 5-coordinate zinc species in MOF-74, as well as the potentially reactive oxo group, may contribute to the highly successful kinetic adsorption. MOF-199 is less successful when challenged with Cl_2 because Cl_2 does not typically act as a ligand. It is clear, however, that MOFs with open metal sites tend to be Lewis acidic and, therefore, highly effective as adsorption media for gases that can act as Lewis bases, which is a weakness in activated carbons (21, 22).

Although open metal sites are reactive electron-deficient groups, amines constitute a common reactive electron-rich group that is available for hydrogen bonding as well. As noted above, the presence of the amine in IRMOF-3 affords a vast improvement relative to MOF-5 in adsorption of NH_3, a molecule that readily forms hydrogen bonds. Relative to BPL carbon, IRMOF-3 adsorbs almost 71 times as much ammonia before breakthrough. Furthermore, IRMOF-3 is observed to outperform BPL carbon by a factor of 1.76 in adsorption of chlorine, against which the open metal site MOFs were ineffective. Clearly it is possible to adsorb a range of contaminants that will react either as Lewis acids or Lewis bases simply by including a reactive functionality of the opposite functionality in a MOF structure.

Some insight into the adsorption mechanism in MOFs can be gleaned by observing changes of color after adsorption of the contaminants. Activated MOF-199 is deep violet in color. After exposure to the atmosphere, its color rapidly changes to light blue, because water molecules coordinate to the open copper site. An identical color change is observed after adsorption of ammonia, indicating that a similar adsorption process is occurring. The color change progresses through the adsorbent bed, clearly indicating the progress of the ammonia front. The change is not reversed by prolonged flow of pure nitrogen, indicating that ammonia molecules have chemisorbed to the copper site. Similar color changes are observed after exposure of MOF-74 to sulfur dioxide, IRMOF-3 to chlorine and ammonia, and IRMOF-62 to chlorine, each of which does not undergo a color change after exposure to atmosphere. In each case the color change clearly indicates the progression of the contaminant front through the adsorbent bed and is not reversed by pure nitrogen flow. Observation of the adsorption process as a color change in the adsorbent is a possibility for MOFs that does not exist for BPL carbon. It provides insight into the binding mechanism and gives a clear indication of the extent of saturation of the adsorbent.

Capture of Vaporous Contaminants. Breakthrough curves for tetrahydrothiophene, benzene, dichloromethane, and ethylene oxide were recorded by using the benchmark MOFs and BPL carbon. Plots of the breakthrough curves and estimated dynamic adsorption capacities for gaseous contaminants are presented in Fig. 3 and Table 2, respectively.

In following with the results of breakthrough experiments on gaseous contaminants, MOF-5 and MOF-177 do not perform well as kinetic adsorption media. IRMOF-62 is also largely outclassed by BPL carbon except in the case of ethylene oxide adsorption, for which IRMOF-62 and BPL carbon are equally ineffective. We also observe that IRMOF-3 is a poor adsorbent for the vapors chosen, because none of them behave as good Lewis acids.

Open metal sites, particularly the copper sites found in MOF-199, prove to be the most effective in removing vapors from the gas stream. Both MOF-74 and MOF-199 outperform BPL carbon by an order of magnitude. However, MOF-74 is not effective against the entire range of vapors, whereas MOF-199 is effective. There is essentially no difference in performance

Table 2. Dynamic adsorption capacities of the benchmark MOFs for gaseous contaminants measured in grams of gas per gram of adsorbent

Gas	MOF-5	IRMOF-3	MOF-74	MOF-177	MOF-199	IRMOF-62	BPL carbon	Improvement factor*
Sulfur dioxide	0.001	0.006	0.194†	<0.001	0.032	<0.001	0.033	5.88
Ammonia	0.006	0.105†	0.093	0.042	0.087	0.023	0.001	105
Chlorine	‡	0.335†	‡	<0.001	0.036	0.092	0.190	1.76
Tetrahydrothiophene	0.001	0.007	0.090	<0.001	0.351†	0.084	0.123	2.85
Benzene	0.002	0.056	0.096	0.001	0.176†	0.109	0.155	1.14
Dichloromethane	<0.001	0.001	0.032	<0.001	0.055†	0.019	0.053	1.04
Ethylene oxide	0.001	0.002	0.110	<0.001	0.095†	0.011	0.010	9.50

*Expresses the ratio of dynamic adsorption capacity of the best-performing MOF (†) to that of BPL carbon.
†Best-performing MOFs.
‡Experiments were not performed because of corrosion of the apparatus by chlorine.

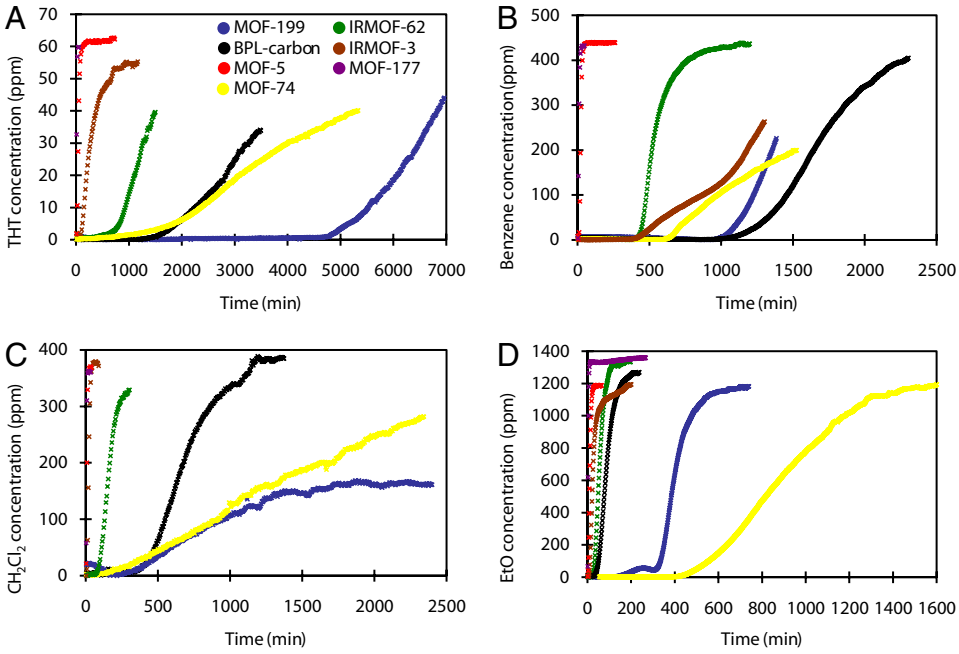

Fig. 3. Breakthrough curves of vaporous tetrahydrothiophene (*A*), benzene (*B*), dichloromethane (*C*), and ethylene oxide (*D*) in the benchmark MOFs. THT, tetrahydrothiophene; EtO, ethylene oxide.

between the activated carbon and MOF-199 in dichloromethane adsorption. There is some improvement over BPL carbon in benzene adsorption and improvement by nearly a factor of 3 in adsorption of tetrahydrothiophene. In each case except for dichloromethane, MOF-199 exhibits a color change identical to that observed after exposure to water or ammonia, again indicating a strong interaction with the open copper site.

Conclusions

Coordinatively unsaturated metal sites (MOF-74 and MOF-199) and amino functionality (IRMOF-3) prove effective in adsorbing contaminants that interact strongly with those groups. In particular, MOF-199 demonstrates efficacy equal to or greater than BPL carbon against all gases and vapors tested except chlorine. It is particularly effective in removing gases that are vexing for activated carbons, such as ammonia and ethylene oxide. Carbon monoxide cannot be captured effectively with any of the MOFs tested in this study.

It is clear that a successful dynamic adsorption medium will contain some reactive functionality, often in the form of a coordinatively unsaturated metal site. A variety of MOFs with reactive functionality in the pores is known, and there exists immense potential for the development of new MOFs with untested functionalities and metals. Furthermore, the performance of any MOF stands to be improved dramatically once it is impregnated with reactive ions and compounds.

Although the findings reported here advance MOFs as promising adsorption media, there remains significant room for additional study. Many applications involve capture of gaseous compounds from mixtures containing potentially reactive impurities or residual humidity. The effect of impurities present in a particular setting on both the structure of a MOF adsorbent and on the binding affinity of the target adsorbate must be addressed. In addition, applications pertaining to personal protection depend on the irreversibility of adsorbate binding. The irreversible color change we report for some adsorbate/MOF pairings serves as evidence of irreversibility, which for protective applications is often desirable. However, for other applications such as gas storage, MOFs are known to bind guests reversibly (5). In summary, our results open up an area of inquiry in the field of MOFs and indicate their great potential to supplement and eventually replace activated carbons as dynamic adsorption media.

Materials and Methods

Preparation of MOFs. MOFs were prepared and activated in bulk quantities by using procedures modified from the literature (5, 9, 10, 23–25). For detailed synthetic procedures for all MOFs, see the *SI Appendix*. Each sample was characterized by powder x-ray (Cu Kα) diffraction and N_2 adsorption isotherm. Apparent surface areas were determined by the BET method and were commensurate with reported values. MOFs were stored under an inert atmosphere.

Breakthrough Testing. A schematic representation of the breakthrough test systems can be found in the *SI Appendix* and Fig. S3. Gasses were purchased from Lehner and Martin, Airgas, and Scott-Marrin as certified mixtures in a balance of N_2, Cl_2 at 4%, CO at 1.05%, SO_2 at 1.00%, and NH_3 at 0.99%. The flow rate was monitored by using a Gilmont rotameter and held at 25 ml/min. Experiments were carried out with the adsorbent at room temperature (25°C). Detection of the effluent gas from the sample was performed by using a Hiden Analytical HPR20 mass spectrometer. Concentrations of N_2, O_2, and the contaminant gas were sampled continuously at a minimum rate of 3 points per min. The concentration of the contaminant gas was calibrated by comparing it to the concentration recorded by the mass spectrometer under unimpeded flow of the source mixture.

Liquid vapors were generated in a balance of nitrogen by a Vici Metronics Dynacalibrator model 230 vapor generator, which is capable of delivering a vapor concentration with ±2% precision. A constant flow rate of 79 ml/min was generated by the vapor generator. The gasses generated for the experiments were mixtures in nitrogen of 64 ppm tetrahydrothiophene, 1,240 ppm ethylene oxide, 440 ppm benzene, and 380 ppm methylene chloride. Experiments were carried out with the adsorbent at 25°C. Detection of the effluent gas from the sample was performed by using a Thermo-Fisher Antaris IGS Fourier-transform infrared spectrometer. The spectrometer was calibrated for detection of each contaminant vapor by using the TQAnalyst software package with a minimum of 16 calibration points across the operating detection range. The concentration of the contaminant vapor was sampled continuously at a minimum rate of 3 points per min.

All experiments were carried out by using a fritted 1.6-cm-i.d. glass sample tube. A bed of MOF 1.0 cm in height (0.4 cm in the case of tetrahydrothiophene tests) was deposited onto the glass frit under inert atmosphere. All samples

were purged with ultrahigh-purity N_2 gas for 20 min before testing. Testing was carried out with the sample cell at room temperature (25°C).

Dynamic Adsorption Capacity. In each experiment, the ''breakthrough concentration'' for each contaminant is defined as 5% of the feed concentration. The time at which the concentration of contaminant gas in the effluent surpasses the breakthrough concentration is designated as the ''breakthrough time.'' The dynamic adsorption capacity is calculated in each case by dividing the total mass of gas adsorbed before breakthrough by the mass of adsorbent.

ACKNOWLEDGMENTS. We gratefully acknowledge the advice of Drs. Christopher Karwacki and Gregory Peterson as well as Iris Rauda, Selma Duhovic, Lisa Dudek, and Chain Lee (Yaghi group members) for preparing bulk samples of the benchmark MOFs. This work was supported by Joint Science and Technology Office of the Department of Defense Project W911NF-06-1-0405.

1. McAtee M, *et al*. (2003) *Chemical Exposure Guidelines for Deployed Military Personnel*, eds Hauschild V, Johnson J (US Army Center for Health Promotion and Preventive Medicine, Aberdeen Proving Ground, MD), Reference document 230. pp 96–113.
2. Peterson GW, Karwacki CJ, Feaver WB, Rossin JA (2008) H-ZSM-5 for the removal of ethylene oxide: Effects of water on filtration performance. *Ind Eng Chem Res* 47:185–191.
3. Petit C, Karwacki C, Peterson G, Bandosz TJ (2007) Interactions of ammonia with the surface of microporous carbon impregnated with transition metal chlorides. *J Phys Chem C Nanomater Interfaces* 111:12705–12714.
4. Wood GO (1992) Activated carbon adsorption capacities for vapors. *Carbon N Y* 30:593–599.
5. Li H, Eddaoudi M, O'Keeffe M, Yaghi OM (1999) Design and synthesis of an exceptionally stable and highly porous metal-organic framework. *Nature* 402:276–279.
6. Rowsell J, Yaghi OM (2004) Metal-organic frameworks: A new class of porous materials. *Microporous Mesoporous Mater* 73:3–14.
7. Yaghi OM, *et al*. (2003) Reticular synthesis and the design of new materials. *Nature* 423:705–714.
8. Eddaoudi M, *et al*. (2001) Modular chemistry: Secondary building units as a basis for the design of highly porous and robust metal-organic carboxylate frameworks. *Acc Chem Res* 34:319–330.
9. Chae H, *et al*. (2004) A route to high surface area, porosity and inclusion of large molecules in crystals. *Nature* 427:523–527.
10. Eddaoudi M, *et al*. (2002) Systematic design of pore size and functionality in isoreticular metal-organic frameworks and application in methane storage. *Science* 295:469–472.
11. Rosi N, *et al*. (2003) Hydrogen storage in microporous metal-organic frameworks. *Science* 300:1127–1129.
12. Duren T, Sarkisov L, Yaghi OM, Snurr RQ (2004) Design of new materials for methane storage. *Langmuir* 20:2683–2689.
13. Rowsell J, Millward A, Park K, Yaghi OM (2004) Hydrogen sorption in functionalized metal-organic frameworks. *J Am Chem Soc* 126:5666–5667.
14. Chen B, Contreras DS, Ockwig N, Yaghi OM (2005) High H_2 adsorption in a microporous metal-organic framework with open-metal sites. *Angew Chem Int Ed* 2005:4745–4749.
15. Rowsell J, Eckert J, Yaghi OM (2006) Characterization of H_2 binding sites in prototypical metal-organic frameworks by inelastic neutron scattering. *J Am Chem Soc* 127:14904–14910.
16. Millward A, Yaghi OM (2006) Metal-organic frameworks with exceptionally high capacity for storage of carbon dioxide at room temperature. *J Am Chem Soc* 127:17998–17999.
17. Furukawa H, Miller M, Yaghi OM (2007) Independent verification of the saturation hydrogen uptake in MOF-177 and establishment of a benchmark for hydrogen adsorption in metal-organic frameworks. *J Mater Chem* 17:3197–3204.
18. Kaye SS, Dailly A, Yaghi OM, Long JR (2007) Impact of preparation and handling on the hydrogen storage properties of Zn_4O(1,4-benzenedicarboxylate)$_3$ (MOF-5). *J Am Chem Soc* 129:14176–14177.
19. Walton KS, *et al*. (2008) Understanding inflections and steps in carbon dioxide adsorption isotherms in metal-organic frameworks. *J Am Chem Soc* 130:406–407.
20. Wood GO, Stampfer JF (1993) Adsorption rate coefficients for gases and vapors on activated carbons. *Carbon* 31:195–200.
21. Horike S, Dinca M, Tamaki K, Long JR (2008) Size-selective Lewis acid catalysis in a microporous metal-organic framework with exposed Mn^{2+} coordination sites. *J Am Chem Soc* 130:5854–5855.
22. Chen BL, Eddaoudi M, Reineke T, O'Keeffe M, Yaghi OM (2000) Cu_2(ATC)·6H_2O: Design of open metal sites in porous metal-organic crystals (ATC: 1,3,5,7-adamantane tetracarboxylate). *J Am Chem Soc* 122:11559–11560.
23. Rowsell J, Yaghi OM (2006) Effects of functionalization, catenation, and variation of the metal oxide and organic linking units on the low-pressure hydrogen adsorption properties of metal-organic frameworks. *J Am Chem Soc* 128:1304–1315.
24. Tranchemontagne D (2007) The Synthesis and Investigation of Alkyne-Containing Isoreticular Metal–Organic Frameworks for Hydrogen Storage and the Preliminary Investigation of Metal–Organic Frameworks for Gas Separation Applications, PhD thesis (Univ of California, Los Angeles).
25. Chui SSY, Lo SMF, Charmant JPH, Orpen AG, Williams ID (1999) A chemically functionalizable nanoporous material [$Cu_3(TMA)_2(H_2O)_3]_n$. *Science* 283:1148–1150.